Relativistic description of the $np \rightarrow \eta d$ reaction near threshold

H. Garcilazo[1] and M. T. Peña[2]

[1]*Escuela Superior de Física y Matemáticas Instituto Politécnico Nacional, Edificio 9, 07738 México D.F., Mexico*
[2]*Instituto Superior Técnico, Centro de Física das Interacções Fundamentais,*
and Department of Physics, Av. Rovisco Pais, P-1049-001 Lisboa, Portugal

Relativistic effects in a three-body calculation of the $np \rightarrow \eta d$ process are considered. Parametrizations for the ηN interaction obtained from phenomenological meson-nucleon models are probed. Relativistic effects on the range and strength of the pion exchange contribution to the reaction mechanism are seen to be large, while boost effects of the two-body interactions are negligible. The relativistic calculation confirms previous nonrelativistic results, showing that the shape of the cross section near threshold is essentially determined by the ηd final-state interaction alone. As for the region away from threshold, the relativistic pion exchange contribution is seen to dominate the other mechanisms of the reaction. It turns out that, within the relativistic reaction model, the $np \rightarrow \eta d$ experimental data call for a comprehensive study to find parameters of the meson-nucleon interactions which are consistent with η production, both on the nucleon as well as on the deuteron.

I. INTRODUCTION

We investigate relativistic effects in the reaction $np \rightarrow \eta d$, in a calculation that considers the ηd final-state three-body distortion. The inclusion of this interaction is crucial for the interpretation of the observed behavior of the cross section at threshold [1,2]. In previous works [3–5] we concluded that the shape of the cross section very near threshold is indeed determined by the three-body nature of the final state interaction. Those calculations were, however, made within a nonrelativistic formalism.

Given the high threshold energy for η production, the inclusion of relativity in the calculation of the $np \rightarrow \eta d$ cross section needs to be pursued. Moreover, it is known that there is a considerable dispersion of the empirical values for the ηN scattering length $a_{\eta N}$ originated by different data analyses. This uncertainty spreads from values for the real part of $a_{\eta N}$ as Re $(a_{\eta N}) = 0.20$ fm, from a calculation of η and K photoproduction in Ref. [6], to values as 0.55 fm, from a calculation of the $pd \rightarrow \eta^3$He reaction in Ref. [7], to even the large values in the $0.72 - 1.07$ fm range, from analysis of the $\pi N - \pi N, \pi N - \eta N \ \pi N - \gamma N$ transition amplitudes in Refs. [8–11]. More recently a model from the Julich group, based on a coupled channel formalism, led to the value Re $(a_{\eta N}) = 0.42$ fm [12]. Therefore, relativistic effects have to be considered to narrow the large uncertainty region for that scattering length. Importantly, the knowledge of this strength is crucial to establish or confirm the possibility for exotic eta-mesic nuclei or nuclear matter, of great astrophysics interest.

Here we introduce and solve a relativistic formalism with the following features:

(i) On one hand, covariant meson-nucleon amplitudes based on different data analyses [8–12] of the coupled reactions $\pi N \rightarrow \eta N, \eta N \rightarrow \eta N$, and $\gamma N \rightarrow \eta N$ are constructed for the first time. The covariant meson-nucleon amplitudes are moreover conveniently boosted (including their Dirac spin structure) to be embedded in the meson production mechanism

through which the reaction proceeds. This mechanism is the meson-exchange box diagram with the excitation of the S_{11} resonance, represented in Fig. 1.

(ii) On the other hand, for the calculation of the ηd final-state distortion, a relativistic version of the three-body equations is used here, which incorporates relativistic kinematics and the boost of the two-body meson-nucleon and nucleon-nucleon interactions. The boost effects are assessed.

The next section describes the formalism. In Sec. II A the relativistic meson-exchange driving term is introduced and in Sec. II B the three-body relativistic formalism for the ηd final state interaction is addressed. In Sec. III the results are shown and discussed. Section IV summarizes the conclusions.

II. FORMALISM

A. The covariant $np \rightarrow \eta d$ box diagram

We will start our discussion with the box diagram shown in Fig. 1 which, together with the impulse term, has been considered as the basic production mechanism [4,5,13–15].

If one evaluates this Feynman diagram by putting the spectator nucleon in the intermediate state on-its-mass-shell, the four-dimensional integral reduces to the integration in the three-momentum $\vec{p}_N$ of that nucleon as

$$A^{\mu_1 \mu_2}_{M_d} = \frac{1}{(2\pi)^3} \sum_\mu \int d\vec{p}_N \frac{M}{E_N} \bar{v}^\mu_N V^{M_d}_{dNN} \frac{p_3 + M}{p_3^2 - M^2} t_{mN \rightarrow \eta N} u^{\mu_2}_2$$

$$\times \frac{1}{k_m^2 - m_m^2} \bar{u}^\mu_N V_{mNN} u^{\mu_1}_1, \qquad (1)$$

where $V^{M_d}_{dNN}$, V_{mNN}, and $t_{mN \rightarrow \eta N}$ are, respectively, the deuteron-nucleon-nucleon vertex, the m meson-nucleon-nucleon vertex, and the meson-nucleon $\rightarrow \eta$ nucleon t matrix. The spinors $u^{\mu_1}_1, u^{\mu_2}_2, u^\mu_N$, correspond, respectively, to the two initial and the intermediate nucleon spinors, and $\bar{v}^\mu_N$ is the
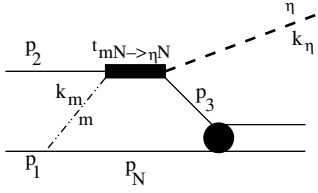
FIG. 1. Meson-exchange mechanism for the reaction $np \to \eta d$.

charged-conjugated spinor. The three-momentum variables are defined as shown on the diagram of Fig. 1.

One expects the effect of relativity to be important in the left-hand side of the box diagram where the exchanged meson m is very far-off-the-mass-shell. However, on the right-hand side of the diagram the final η is restricted to the energy region of $E < 100$ MeV, so that the effects of relativity are not so crucial. Therefore, we will write the propagator for the intermediate nucleon in terms of positive and negative energy spinors and keep only the positive energy part:

$$
\begin{aligned}
\frac{\not{p}_3 + M}{p_3^2 - M^2} &= \frac{M}{E_3} \sum_{\mu_3} \frac{u_3^{\mu_3}(\vec{p}_3) \bar{u}_3^{\mu_3}(\vec{p}_3)}{p_{03} - E_3} \\
&+ \frac{M}{E_3} \sum_{\mu_3} \frac{v_3^{\mu_3}(-\vec{p}_3) \bar{v}_3^{\mu_3}(-\vec{p}_3)}{p_{03} + E_3} \\
&\to \frac{M}{E_3} \sum_{\mu_3} \frac{u_3^{\mu_3}(\vec{p}_3) \bar{u}_{\mu_3}^3(\vec{p}_3)}{p_{03} - E_3}.
\end{aligned} \tag{2}
$$

If we now consider the deuteron wave function $\Psi_{M_d, \mu\mu_3}^*(\vec{p})$ defined by the identification that is valid in the rest frame of the deuteron (which in the region near threshold is very near the ηd rest frame) [16]

$$
\begin{aligned}
&\frac{M}{E_3} \bar{v}_N^\mu(\vec{p}_N) V_{dNN}^{M_d} u_3^{\mu_3}(\vec{p}_3) \frac{1}{p_{03} - E_3} \\
&\equiv \sqrt{2\omega_d}(2\pi)^{3/2} \Psi_{M_d, \mu\mu_3}^*(\vec{p}),
\end{aligned} \tag{3}
$$

where $\vec{p}$ is the NN relative momentum in the center of mass (c.m.), we obtain from Eq. (1)

$$
\begin{aligned}
A_{M_d}^{\mu_1 \mu_2} &= \frac{1}{(2\pi)^{3/2}} \sum_{\mu, \mu_3} \int d\vec{p}_N \frac{M}{E_N} \sqrt{2\omega_d} \Psi_{M_d, \mu\mu_3}^*(\vec{p}) \\
&\times \bar{u}_3^{\mu_3}(p_3) t_{mN \to \eta N} u_2^{\mu_2}(p_2) \frac{1}{p_m^2 - m_m^2} \\
&\times \bar{u}_N^\mu(p_N) V_{mNN} u_1^{\mu_1}(p_1).
\end{aligned} \tag{4}
$$

In Eq. (4) we made explicit the momentum dependence of the nucleon spinors.

The deuteron wave function is on the other hand calculated from

$$
\Psi_{M_d, \mu\mu_3}^*(\vec{p}) = \sum_{L=0,2} \sum_{m_L, m_S} C_{m_L \ m_S \ M_d}^{L \ 1 \ 1} \phi_L(p) Y_{Lm_L}^*(\hat{p}) C_{\mu \ \mu_3, \ m_S}^{1/2 \ 1/2 \ 1}, \tag{5}
$$

where $\phi_0(p)$ and $\phi_2(p)$ are the S- and D-wave components which we obtained from the Paris potential.

For the m meson-nucleon-nucleon vertex we take

$$
V_{mNN} = g_m \gamma_5 f_m(k_m^2), \quad m = \pi, \eta, \tag{6}
$$

and

$$
V_{mNN} = g_m f_m(k_m^2), \quad m = \sigma, \tag{7}
$$

where k_m^2 is the meson four-momentum squared and the form factor f_m is chosen to have the monopole form

$$
f_m(k_m^2) = \frac{\Lambda^2 - m_m^2}{\Lambda^2 - k_m^2}, \tag{8}
$$

with $\Lambda = 1800$ MeV/c which is a typical value for meson-exchange models [17,18].

Since the η production near threshold is dominated by the S_{11} resonance, the m meson-nucleon $\to \eta$-nucleon t transition operator is assumed to be generated by a variable-mass isobar model consisting of a single isobar, the S_{11}. As in the framework introduced in Ref. [19] for the study of the pion induced eta production reaction, the isobar model for meson-nucleon scattering used here is covariant, and reads

$$
\begin{aligned}
&t_{mN \to \eta N}(\vec{p}^2, \vec{p}'^2, M_S) \\
&= \frac{(2\pi)^2}{M} \sqrt{\omega_m(\vec{p}^2) \omega_\eta(\vec{p}'^2) E_N(\vec{p}^2) E_N(\vec{p}'^2)} \\
&\times h_m(\vec{p}^2) \frac{\not{k}_N + \not{k}_2 + M_S}{2M_S} h_\eta(\vec{p}'^2) \tau(M_S),
\end{aligned} \tag{9}
$$

where $\omega_m(\vec{p}^2) = \sqrt{m_m^2 + \vec{p}^2}$, $E_N(\vec{p}^2) = \sqrt{M^2 + \vec{p}^2}$ are the on-shell energies, respectively, of the m meson and of the nucleon in the c.m. frame. Also one has

$$
M_S = \sqrt{(k_m + k_2)^2} = \sqrt{(k_\eta + k_3)^2}. \tag{10}
$$

The meson-nucleon-isobar vertices are

$$
h_m(\vec{p}^2) = \sqrt{\frac{2M}{M + E_N(\vec{p})}} g_m(\vec{p}^2), \quad m = \pi, \eta, \tag{11}
$$

and

$$
h_m(\vec{p}^2) = \frac{M}{\sqrt{\vec{p}^2}} \sqrt{\frac{2M}{M + E_N(\vec{p})}} g_m(\vec{p}^2) \gamma_5, \quad m = \sigma. \tag{12}
$$

Here, three-momentum squared $\vec{p}^2$ ($\vec{p}'^2$) is the meson-nucleon relative initial (final) three-momentum in the c.m. frame. In particular, it is related to Lorentz invariant quantities as

$$
\vec{p}^2 = \frac{(M_S^2 + M^2 - k_m^2)^2}{4M_S^2} - M^2. \tag{13}
$$

The isobar propagator $\tau(M_S)$ is obtained from a separable potential model describing the coupled $\eta N - \pi N - \sigma N$ two-body subsystem. The corresponding two-body t matrix (9) is also separable in any reference frame. We note that the σN channel stands for the $\pi \pi N$ inelasticity. Also, in variance with Ref. [20] we do not consider ρ exchange. Recently in Ref. [14] it was shown that the exact numerical treatment of the initial state interaction reduces significantly the ρ-exchange diagram, relative to the other meson exchanges.

In the basis states of the nucleon spinors the matrix element of the transition operator on Eq. (9) in the two-body

meson-nucleon c.m. system, where $\vec{k}_m + \vec{k}_2 = \vec{k}_\eta + \vec{k}_3 = 0$, is given by

$$\bar{u}_3^{\mu_3} t_{mN \to \eta N} u_2^{\mu_2} = \frac{2\pi}{M} \delta_{\mu_2 \mu_3} \sqrt{\omega_m(\vec{p}^2) \omega_\eta(\vec{p}'^2) E_N(\vec{p}^2) E_N(\vec{p}'^2)}$$

$$\times g_m(\vec{p}^2) \tau(M_S) g_\eta(\vec{p}'^2), \qquad (14)$$

and a completely similar expression in the case of the transition $mN \to m'N$ with m or m' any of the three mesons.

We consider nucleon 2 with momentum $\vec{q}_N$ in the positive direction of the z axis and the η meson three-momentum in the xz plane with polar angle θ. Then the amplitude A of Eq. (4) satisfies the symmetry property

$$A_M^{\mu_1 \mu_2}(\vec{q}_N, \theta) = -(-1)^{M+\mu_1+\mu_2} A_M^{\mu_1 \mu_2}(-\vec{q}_N, \pi - \theta). \qquad (15)$$

In the isospin formalism the neutron and proton are identical particles, so that the initial np state must be antisymmetrized under the exchange of nucleons 1 and 2. However, the system is in a pure total isospin-0 state, which means that the initial np state must be symmetric under the exchange of space and spin variables. Therefore, the correctly antisymmetrized amplitude $\bar{A}_M^{\mu_1 \mu_2}$ for the $np \to \eta d$ process is

$$\bar{A}_M^{\mu_1 \mu_2} = \frac{1}{\sqrt{2}} \left[A_M^{\mu_1 \mu_2}(\vec{q}_N, \theta) + A_M^{\mu_2 \mu_1}(-\vec{q}_N, \theta) \right]$$

$$= \frac{1}{\sqrt{2}} \left[A_M^{\mu_1 \mu_2}(\vec{q}_N, \theta) - (-1)^{M+\mu_1+\mu_2} A_M^{\mu_2 \mu_1}(\vec{q}_N, \pi - \theta) \right]. \qquad (16)$$

B. The ηd scattering and the boost of the two-body interactions

In our previous work [5] we presented the formalism to calculate ηd scattering based on nonrelativistic Faddeev equations. Since we are now discussing relativistic effects in the $np \to \eta d$ process, it becomes necessary to perform here also a relativistic calculation of the ηd elastic channel responsible for the final-state interaction in the $np \to \eta d$ reaction. To generate the necessary ηd distorted waves, we apply to the ηd elastic channel the relativistic formalism in momentum space presented in Ref. [21]. This formalism generalizes in a straightforward way the nonrelativistic Faddeev equations. It incorporates relativistic kinematics and, importantly, also the boosts of the two-body interactions to the three-body c.m. frame. Since the energies that we consider in this work are in the continuum, we deal with the three-body singularities by using the method of contour rotation [22].

Firstly, the main feature of the formalism of [21] consists of a set of relativistic but three-dimensional integral Faddeev-type equations obtained from a field theory in which the three particles are kept on their mass shell in all intermediate states. Accordingly, in what follows the quantity k_i does not refer to the four-momentum of particle i, but to the magnitude of its three-momentum $\vec{k}_i$. Secondly, in order to transform correctly all physical quantities from the two-body to the three-body reference frames, and after considering the energy conservation constraint, one writes the invariant momentum space volume element for the three particles in terms of the

two relative Jacobi variables $\vec{p}_i$ and $\vec{q}_i$,

$$dV = \frac{d\vec{k}_1}{2\omega_1(k_1)} \frac{d\vec{k}_2}{2\omega_2(k_2)} \frac{d\vec{k}_3}{2\omega_3(k_3)} \delta(\vec{k}_1 + \vec{k}_2 + \vec{k}_3)$$

$$= \frac{\omega(p_i)}{8 W_i(p_i q_i) \omega_i(q_i) \omega_j(p_i) \omega_k(p_i)} d\vec{p}_i d\vec{q}_i. \qquad (17)$$

The variable $\vec{p}_i$ is the relative momentum of the pair jk measured in the c.m. frame of the pair (that is, the frame in which particle j has momentum $\vec{p}_i$ and particle k has momentum $-\vec{p}_i$), and $\vec{q}_i = -\vec{k}_i$ is the relative momentum between the pair jk and the spectator particle i, measured in the c.m. frame of the three particles, (in which the pair jk has total momentum $\vec{q}_i$ and particle i has momentum $-\vec{q}_i$). The energy of the jk pair in its c.m. frame is

$$\omega(p_i) = \sqrt{m_j^2 + p_i^2} + \sqrt{m_k^2 + p_i^2}, \qquad (18)$$

the total energy of the pair is

$$W_i(p_i q_i) = \sqrt{\omega^2(p_i) + q_i^2}, \qquad (19)$$

and the invariant energy of the three particles is written as

$$W(p_i q_i) = \omega_i(q_i) + W_i(p_i q_i), \qquad (20)$$

with

$$\omega_i(q_i) = \sqrt{m_i^2 + q_i^2}. \qquad (21)$$

Equations (17)–(21) determine the transformation of the matrix elements of the two-body potential V, given in the two-body c.m. frame by $V(\vec{p}_i, \vec{p}'_i)$, to the three-body c.m. reference frame, as found in [21]:

$$\langle \vec{p}_i \vec{q}_i | V | \vec{p}'_i \vec{q}'_i \rangle$$

$$= \left[\frac{W_i(p_i q_i) \omega_j(p_i) \omega_k(p_i) W_i(p'_i q_i) \omega_j(p'_i) \omega_k(p'_i)}{\omega(p_i) \omega(p'_i)} \right]^{1/2}$$

$$\times 8\omega_i(q_i) \delta(\vec{q}_i - \vec{q}'_i) V(\vec{p}_i, \vec{p}'_i), \qquad (22)$$

which in turn defines the boosted matrix elements of the two-body t matrix. These are given by

$$\langle \vec{p}_i \vec{q}_i | t | \vec{p}'_i \vec{q}'_i \rangle$$

$$= \left[\frac{W_i(p_i q_i) \omega_j(p_i) \omega_k(p_i) W_i(p'_i q_i) \omega_j(p'_i) \omega_k(p'_i)}{\omega(p_i) \omega(p'_i)} \right]^{1/2}$$

$$\times 8\omega_i(q_i) \delta(\vec{q}_i - \vec{q}'_i) t(\vec{p}_i, \vec{p}'_i; q_i), \qquad (23)$$

where $t(\vec{p}_i, \vec{p}'_i; q_i)$ satisfies the Lippmann-Schwinger equation with a propagator corresponding to relativistic kinematics defined by Eq. (20):

$$t(\vec{p}_i, \vec{p}'_i; q_i) = V(\vec{p}_i, \vec{p}'_i) + \int d\vec{p}''_i V(\vec{p}_i, \vec{p}''_i)$$

$$\times \frac{1}{W_0 - W(p''_i q_i) + i\epsilon} t(\vec{p}''_i, \vec{p}'_i; q_i). \qquad (24)$$

The variable W_0 is the invariant energy of the system. For only S-wave two-body interactions Eq. (24)

becomes

$$t(p_i, p_i'; q_i) = V(p_i, p_i') + \int_0^\infty p_i''^2 dp_i'' V(p_i, p_i'')$$

$$\times \frac{1}{W_0 - W(p_i''q_i) + i\epsilon} t(p_i'', p_i'; q_i). \quad (25)$$

In the particular case of the coupled $\eta N - \pi N - \sigma N$ subsystem (we take $m_\sigma = 2m_\pi$, since the σN channel simulates the $\pi\pi N$ inelasticity), these three different meson-nucleon channels are connected among each other through the S_{11} partial wave. For each transition, we use rank-one separable potentials of the form

$$V_{mm'}(p_i, p_i') = -g_m(p_i)g_{m'}(p_i'); \quad (m, m' = \eta, \pi, \sigma), \quad (26)$$

where we considered two types of models for the functions g_m. In order to evaluate the sensitivity of the numerical results to the functional form of g_m, we tested two types of functions with different "fall-off" behavior for large values of the momenta: models of type I, with the same form as in Ref. [5],

$$g_m(p_i) = \sqrt{\lambda_m} \frac{A_m + p_i^2}{(\alpha_m^2 + p_i^2)^2}; \quad (m = \eta, \pi), \quad (27)$$

$$g_m(p_i) = \sqrt{\lambda_m} \frac{p_i}{(\alpha_m^2 + p_i^2)^2}; \quad (m = \sigma), \quad (28)$$

and models of type II, which have a tail of gaussian form,

$$g_m(p_i) = \sqrt{\lambda_m} (A_m + p_i^2) e^{-p_i^2/2\alpha_m^2}; \quad (m = \eta, \pi), \quad (29)$$

$$g_m(p_i) = \sqrt{\lambda_m} p_i e^{-p_i^2/2\alpha_m^2}; \quad (m = \sigma). \quad (30)$$

The solution of Eq. (25) for the potential (26) is

$$t_{mm'}(p_i, p_i'; q_i) = g_m(p_i)\tau(W_0, q_i)g_{m'}(p_i'), \quad (31)$$

with

$$\tau^{-1}(W_0, q_i) = -1 - \sum_{m=\eta,\pi,\sigma} \int_0^\infty p_i^2 dp_i \frac{g_m^2(p_i)}{W_0 - W(p_iq_i) + i\epsilon}. \quad (32)$$

On one hand, the energy behavior of the meson-nucleon t matrix in Eq. (31) is determined by the dynamical equation (32) and therefore is not arbitrary. On the other hand, since the fits of the meson-nucleon scattering data test two different types of vertex functions $g_m(p_i)$, we assess the extent of model dependence in the final results obtained.

We will now check the consistency between the result for the boosted two-body t-matrix elements derived in this section, and the result for the covariant two-body matrix elements introduced in the previous section. For that, we take Eq. (23) for $q_i = 0$ and obtain

$$\langle \vec{p}_i \vec{0} | t | \vec{p}_i' \vec{q}_i' \rangle = [\omega_j(p_i)\omega_k(p_i)\omega_j(p_i')\omega_k(p_i')]^{1/2}$$

$$\times 8m_i \delta(\vec{0} - \vec{q}_i') t(\vec{p}_i, \vec{p}_i'; 0). \quad (33)$$

From Eqs. (33) and (14) we conclude that the t-matrix element dynamically generated from the separable potential model of Eq. (26) and the relativistic scattering equation, coincides with the covariant matrix element of Eq. (14) obtained in the basis states of the nucleon spinors. The

different multiplicative factors ($8m_i$ vs $\frac{2\pi}{M}$) originate from the normalization convention for two-body momentum basis states used in Faddeev-type formalisms.

The driving terms of the Faddeev equations for ηd elastic scattering given by Eqs. (20)–(22) of Ref. [5] are here modified by the inclusion of relativistic kinematics. By using the invariant three-body volume element we make the replacement

$$\frac{1}{E - p_j^2/2\mu_j - q_j^2/2\nu_j + i\epsilon}$$

$$\rightarrow \left[\frac{W_i(p_i'q_i)\omega_j(p_i')\omega_k(p_i')W_j(p_jq_j)\omega_k(p_j)\omega_i(p_j)}{\omega(p_i')\omega(p_j)\omega_i(q_i)\omega_j(q_j)} \right]^{1/2}$$

$$\times \frac{1}{\omega_k(q_k)} \frac{1}{W_0 - W(p_jq_j) + i\epsilon}, \quad (34)$$

with p_i', p_j, and $\omega_k(q_k)$ defined by Eqs. (70), (71), and (66) of Ref. [21].

The NN interaction appears in two different ways in the description of the $np \rightarrow \eta d$ reaction. First of all, there is the np initial-state interaction at energies near the η threshold ($T_N \approx 1252$ MeV), which acts mainly in the isospin-0 $^1P_1$ partial wave. Secondly, it appears in the three-body equations which determine the final-state ηd distorted waves, where the NN interaction is needed at energies near threshold ($T_N \approx 0$) and for the isospin-1 $^3S_1$ partial wave.

In the case of the np initial-state interaction we used in Ref. [5] the optical potential

$$V(p, p') = V_{\text{PARIS}}(p, p') - i\gamma \frac{pp'}{(\alpha^2 + p^2)(\alpha^2 + p'^2)}, \quad (35)$$

where the parameters $\gamma = 0.6$ and $\alpha = 0.75$ fm^{-1} were obtained by reproducing the np $^1P_1$ amplitude of Arndt *et al.* [23] at the η threshold within the nonrelativistic Lippmann-Schwinger equation

$$T(p, p') = V(p, p') + \int_0^\infty p''^2 dp'' V(p, p'')$$

$$\times \frac{M}{p_0^2 - p''^2 + i\epsilon} T(p'', p'). \quad (36)$$

Since in this work we are interested on a relativistic description of the process we use instead the relativistic Lippmann-Schwinger equation

$$T(p, p') = V(p, p') + \int_0^\infty p''^2 dp'' V(p, p'')$$

$$\times \frac{1}{2} \frac{1}{\sqrt{M^2 + p_0^2} - \sqrt{M^2 + p''^2} + i\epsilon} T(p'', p'). \quad (37)$$

In addition, we have now used as input the $^1P_1$ amplitude of the most recent analysis of Arndt *et al.* [24] from which we extracted $\gamma = 0.8$ and $\alpha = 0.3$ fm^{-1}.

In the case of the NN interaction that appears in the three-body equations which determine the final-state ηd distorted waves, we used in [5] the PEST separable model of Ref. [25],

$$\langle p | V_{NN} | p' \rangle = -g_N(p)g_N(p'), \quad (38)$$

TABLE I. Parameters of the ηN-πN-σN separable potential models of type I fitted to the S_{11} resonant amplitudes given in Refs. [7–10].

Model	Ref.	$a_{\eta N}$	α_η	A_η	λ_η	α_π	A_π	λ_π	α_σ	λ_σ
0	[12]	0.42 + i0.34	5.85798	7.20057	−202.573	0.384338	0.00306689	−0.0804278	0.808	−0.155061
1	[9]	0.72 + i0.26	29.9983	359.211	−5991.79	2.28053	1.08638	−0.0660518	8.0	−239.860
2	[10]	0.75 + i0.27	6.80695	409.632	−0.0735564	9.17614	1.46599	−701.087	8.0	−816.460
3	[11](D)	0.83 + i0.27	5.43840	74.9154	−0.387884	8.83448	0.449176	−654.504	8.0	−760.560
4	[11](A)	0.87 + i0.27	4.35990	30.3941	−0.376959	8.96712	0.270940	−687.477	8.0	−618.431
5	[11](B)	1.05 + i0.27	2.04950	2.60222	−0.102332	9.71806	0.192626	−849.271	8.0	−236.559
6	[11](C)	1.07 + i0.26	1.99979	2.28184	−0.105698	9.76374	0.0702236	−861.215	8.0	−174.670

where

$$g_N(p) = \sum_{n=1}^{6} \frac{c_n}{\beta_n^2 + p^2}, \qquad (39)$$

with the parameters given in Ref. [25]. This potential when substituted into the nonrelativistic Lippmann-Schwinger equation (36) has a bound-state solution at precisely the energy of the deuteron and its wave function is identical to the $L = 0$ component of the deuteron wave function of the Paris potential. In order to make the potential (38) consistent with the relativistic Lippmann-Schwinger equation (37) we multiplied it by a factor, i.e., the relativistic version of the potential is

$$\langle p|V_{NN}|p' \rangle = -0.78805 g_N(p)g_N(p'), \qquad (40)$$

with $g_N(p)$ given by Eq. (39). The potential (40) when substituted into the relativistic Lippmann-Schwinger equation (37) has a bound-state solution at the energy of the deuteron and its wave function at low momenta coincides with the deuteron wave function of the Paris potential.

As for the ηNN coupling constant, on one hand, it was given the reasonable value $g_\eta^2/4\pi = 1$. This quantity is not well known [26–30]. The nucleon-nucleon potential models, require $2 < g_\eta^2/4\pi < 7$ (Bonn potential models) or $g_\eta^2/4\pi = 0.25$ (Nijmegen potential). The analysis of η photoproduction on the other hand gives $1.0 < g_\eta^2/4\pi < 1.4$, or even smaller values. The light cone sum rule yields $g_\eta^2/4\pi = 0.3 \pm 0.15$. As for the σNN coupling constant we used the value of Ref. [31], $g_\sigma^2/4\pi = 8$. The several meson-nucleon coupled channel $\eta N - \pi N - \sigma N$ models constructed here, on the other hand, probe the wide range of uncertainty for the $\eta - N$ scattering lengths, from the low value Re $(a_{\eta N}) = 0.42$ fm of the Julich model to the larger values in the $0.72 - 1.07$ fm region.

III. RESULTS

We organized this section into four parts. In part A the effect of relativity on the parametrizations of the meson-nucleon models is analyzed. In part B the results for the total cross section are shown and the pion-exchange contribution is discussed. In part C the effects of an exact treatment of the initial NN interaction are presented. In part D the role of a heavy-meson exchange is considered.

A. Comparison between relativistic and nonrelativistic models

We give in Table I the parameters of the seven models of type I, as defined in the previous section, which fit the meson-nucleon amplitude analysis of Refs. [8–12] by Eqs. (31) and (32). In Table II we give the parameters of the models for the same seven empirical amplitudes, but within the parametrization of type II. The quality obtained for the fits to the amplitudes of those analyses is at least as good as the one shown in Fig. 1 in Ref. [5], and therefore we do not repeat the corresponding figure.

Relativistic corrections are contained in the dressed propagator given by Eq. (32). Naturally, the comparison of the nonrelativistic models in Ref. [5] with the relativistic cases presented in this work is more meaningful in the case of the models in group I, since in each model of this group the vertex momentum dependence is the same as in the nonrelativistic corresponding case.

Thus, focusing on the cases in group I, in all with the exception of model 0, the parameters for the σ exchange are the ones that deviate less from the parameters obtained within the nonrelativistic calculation of Ref. [5] and shown therein in Table I. In contrast, due to its small mass, the pion contribution is affected by the relativistic treatment.

TABLE II. Parameters of the ηN-πN-σN separable potential models of type II fitted to the S_{11} resonant amplitudes given in Refs. [7–10].

Model	Ref.	$a_{\eta N}$	α_η	A_η	λ_η	α_π	A_π	λ_π	α_σ	λ_σ
0	[12]	0.42 + i0.34	3.97583	36.5287	−1.37E ×10^{-4}	1.33063	1322.81	−5.17E ×10^{-7}	0.708750	−25.1019
1	[9]	0.72 + i0.26	25.8807	1108.42	−1.27E ×10^{-9}	2.73805	29.8046	−4.9E ×10^{-7}	11.1150	−1.41E ×10^{-5}
2	[10]	0.75 + i0.27	25.7330	1123.75	−1.33E ×10^{-9}	3.48693	0.269374	−1.52E ×10^{-5}	1.52544	−1.42E ×10^{-4}
3	[11](D)	0.83 + i0.27	2.77545	105.509	−3.88E ×10^{-7}	6.18513	0.516560	−2.11E ×10^{-5}	1.21418	−9.09E ×10^{-4}
4	[11](A)	0.87 + i0.27	2.65296	117.486	−3.41E ×10^{-7}	5.828627	0.196750	−2.68E ×10^{-5}	7.71062	−5.85E ×10^{-5}
5	[11](B)	1.05 + i0.27	2.16388	79.4167	−4.88E ×10^{-7}	5.95292	0.100986	−1.43E ×10^{-5}	17.4976	−1.59E ×10^{-5}
6	[11](C)	1.07 + i0.26	2.20109	103.150	−3.56E ×10^{-7}	6.44407	0.0358158	−1.67E ×10^{-5}	8.91135	−1.84E ×10^{-5}

TABLE III. ηd scattering length (in fm) predicted by the seven separable potential models of the coupled ηN-πN-σN system, in both types I and II studied here. We give the results obtained including only η exchange, η and π exchange, and η-π and σ exchange in the driving terms. Comparison with results of Ref. [5] is provided on the lines labeled "NR".

	Model	$a_{\eta N}$	η	$\eta + \pi$	$\eta + \pi + \sigma$
	0 I	$0.42 + i0.34$	$0.88 + i1.34$	$0.39 + i1.67$	$0.23 + i1.68$
	0 II	$0.42 + i0.34$	$0.83 + i1.11$	$0.76 + i1.20$	$0.37 + i1.37$
NR	0	$0.42 + i0.34$	$1.01 + i1.24$	$1.00 + i1.28$	$0.99 + i1.28$
	1 I	$0.72 + i0.26$	$2.59 + i1.84$	$2.67 + i1.90$	$2.67 + i1.90$
	1 II	$0.72 + i0.26$	$2.23 + i1.15$	$2.30 + i1.18$	$2.30 + 1.18$
NR	1	$0.72 + i0.26$	$2.53 + i1.51$	$2.56 + i1.51$	$2.57 + i1.51$
	2 I	$0.75 + i0.27$	$2.73 + i1.66$	$2.78 + i1.68$	$2.78 + i1.68$
	2 II	$0.75 + i0.27$	$2.43 + i1.20$	$2.46 + i1.21$	$2.47 + i1.21$
NR	2	$0.75 + i0.27$	$2.75 + i1.64$	$2.75 + i1.62$	$2.76 + i1.62$
	3 I	$0.83 + i0.27$	$3.23 + i1.88$	$3.28 + i1.91$	$3.29 + i1.91$
	3 II	$0.83 + i0.27$	$3.16 + i1.91$	$3.21 + i1.94$	$3.23 + i1.95$
NR	3	$0.83 + i0.27$	$3.28 + i1.93$	$3.28 + i1.91$	$3.30 + i1.91$
	4 I	$0.87 + i0.27$	$3.45 + i1.92$	$3.50 + i1.95$	$3.51 + i1.95$
	4 II	$0.87 + i0.27$	$3.47 + i1.93$	$3.52 + i1.96$	$3.53 + i1.96$
NR	4	$0.87 + i0.27$	$3.55 + i2.07$	$3.56 + i2.05$	$3.57 + i2.04$
	5 I	$1.05 + i0.27$	$4.72 + i2.47$	$4.80 + i2.52$	$4.80 + i2.52$
	5 II	$1.05 + i0.27$	$4.75 + i2.48$	$4.82 + i2.53$	$4.83 + i2.53$
NR	5	$1.05 + i0.27$	$4.91 + i2.72$	$4.92 + i2.70$	$4.93 + i2.70$
	6 I	$1.07 + i0.26$	$5.00 + i2.54$	$5.09 + i2.60$	$5.09 + i2.60$
	6 II	$1.07 + i0.26$	$4.92 + i2.43$	$5.00 + i2.49$	$5.01 + i2.49$
NR	6	$1.07 + i0.26$	$4.77 + i2.25$	$4.79 + i2.25$	$4.79 + i2.24$

In models 2–6 relativity increases slightly the pion momentum range parameter α_π. But at the same time the pion strength parameter A_π increases. According to Eq. (27), the last parameter defines the weight of the small versus the large momentum region. Therefore the increasing of its magnitude acts in the opposite direction of the increasing range parameter. Since the relativistic fit of the meson-nucleon amplitudes has the quality of the nonrelativistic one, the extra weight of the high momentum tail is verified to compensate the increase of A_π. As for the ηN channel, in the same models 2–6, both the range and strength parameters decrease, allowing also the effects of both variations to act in opposite directions, and to almost cancel out.

However, and still within group I, models 1, and specially model 0, which lead to smaller values for the ηN scattering lengths, behave differently than the other four models described since the pion range is seen to decrease. Moreover, for model 0 the pion low-momentum strength A_π uniquely decreases more, percentagewise, than the range parameter α_π. As a net result the weight of the high momentum range versus the low momentum range is increased. Within group II, model 0 is singled out from the other models by its small values for the pion range α_π and strength A_π.

The relative weight between small and large momenta in the meson-nucleon interaction directly reflects on the behavior of the three-body ηd system, and consequently also on the cross section for $np \rightarrow \eta d$, as we will see next. In order to show this, first, we turn now to the results obtained for the ηd three-body elastic channel. We give in Table III the predictions

for the three-body ηd scattering length obtained using the seven two-body $\eta N - \pi N - \sigma N$ coupled interaction models in both groups I and II. We present the results corresponding to the box diagram in Fig. 1 as driving term of the Faddeev equations (see Fig. 3 of Ref. [5] for their diagrammatic representation) including the different meson-exchanges, one by one, in successive cumulative steps: only η exchange, $\eta + \pi$ exchange, or $\eta + \pi + \sigma$ exchange.

To conclude about the extent of the relativistic effects we show for each model the nonrelativistic results of [5] (lines labeled "NR"). As expected, the effect of the relativistic treatment on the three-body scattering length is clearly seen to be more accentuated in the contribution of the pion, which is the lightest meson. Its contribution to the three-body scattering length is negligible in all nonrelativistic models [5]. Compared with the corresponding results of [5], the relativistic results are still quite similar to those of the nonrelativistic case, with the exception of model 0, in the case of group I. The pion exchange contribution to the scattering length is now quite important in the case of this model. This happens because in model 0 in group I, the relativistic changes in the range α_π parameter do not compensate for the changes in the low-momentum strength A_π parameter, as it happens in the other models of that group. As for model 0 in group II, the comparison with the nonrelativistic case is not direct due to different functional forms of the meson-nucleon interactions, but nevertheless we note that the parametrization II of model 0 cuts the high momentum tail such that the pion exchange contribution is closer to the nonrelativistic case.
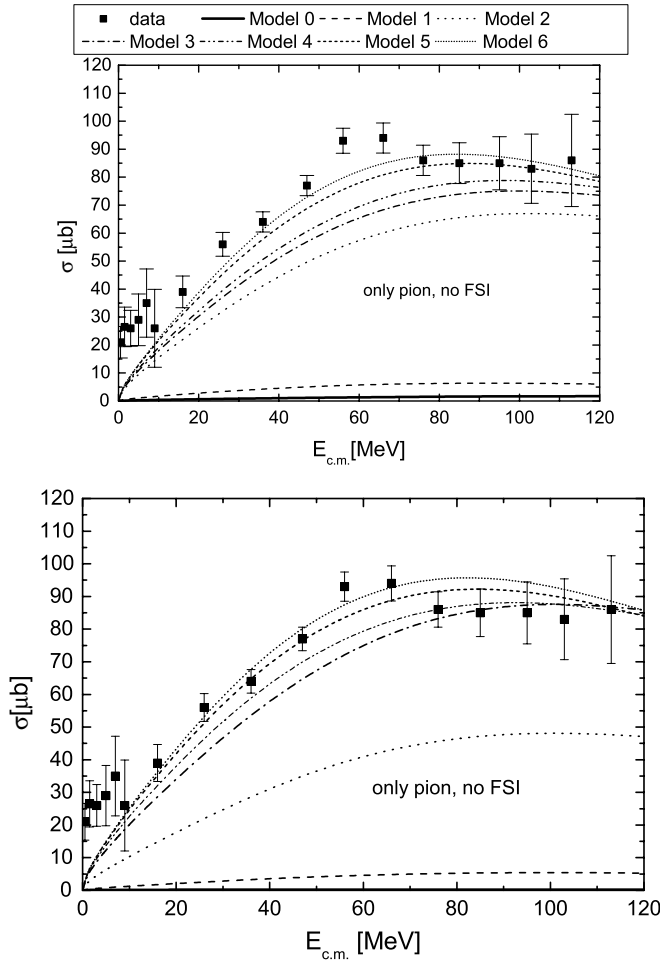
FIG. 2. Total cross section of the reaction $np \to \eta d$ for the seven relativistic meson-nucleon interaction models considered. Only pion exchange is considered in the box diagram represented by Fig. 1. No ηd final state interaction included. The initial state distortion is described by multiplication by a constant factor of 0.2. Data are from Refs. [1,2]. Models I (II) are shown on the top (bottom) panel.

FIG. 3. The same as Fig. 2, but with inclusion of π, η, and σ exchanges in the diagram represented by Fig. 1.

Besides the changes that the relativistic two-body models induce on the pion exchange contribution, the comparison done on Table III gives also indirect information on the magnitude of the boosts of the two-body interactions within the three-body system. Given the agreement in the three-body calculation of the ηd scattering length observed for most cases between the relativistic and nonrelativistic version of the models, boost effects do not appear relevant. Since the energies involved ($\sim$100 MeV) are much smaller than the masses of the η and the nucleon, this is expected.

To summarize, the relativistic effects on the parameters of the two-body meson-nucleon interactions are large, but the boost effects in the three-body system small.

B. Results for the cross section

In this section we compare the results obtained for the cross section by the several models. In all figures of this section the upper panel refers to the models of type I, while the
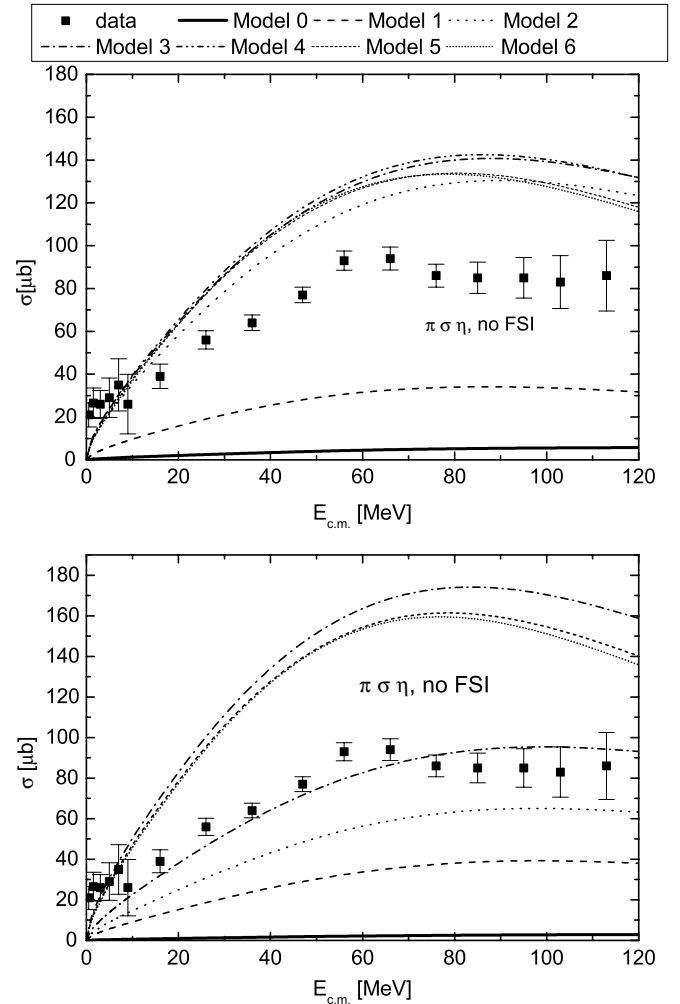
bottom panel is for models of type II, and a reduction factor of 5 corresponding to the initial-state NN interaction was introduced as derived in [5]. This last aspect will be improved upon in the next section.

We show in Fig. 2 the cross section of the $np \to \eta d$ process when only pion exchange is included in the box diagram (see Fig. 1) and **no** final-state interaction is included.

Although models 2–6 (those with a large ηN scattering length) predict more or less the right magnitude for the cross section at large energies, near threshold all models fail to reproduce the enhancement shown by the data. We notice that the models with larger absolute pion strength λ_π and smaller absolute η strength λ_η are closer to the data away from threshold. This result is consistent with only small momentum transfer being needed in this energy region, and is henceforth common to group I and group II.

We show in Fig. 3 the corresponding results when in addition the contribution of the exchanges of the η and σ mesons are included in the box diagram. From both Figs. 2 and 3 it is clear that the dominant exchange mechanism for the $np \to \eta d$ process is pion exchange. This conclusion
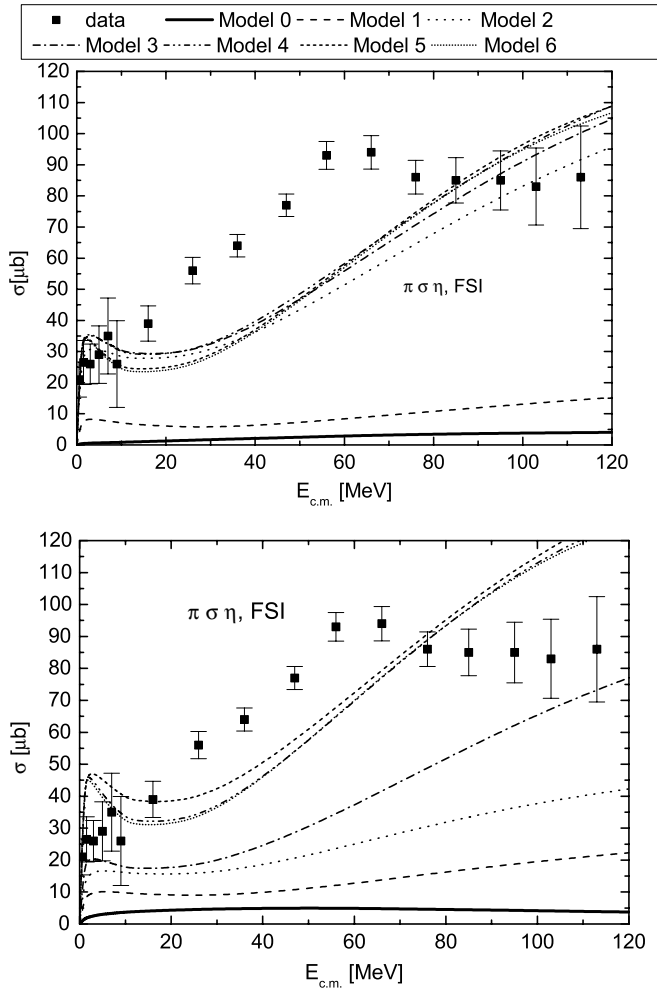
FIG. 4. The same as Fig. 3, but with the inclusion of ηd final state interaction.

FIG. 5. The same as Fig. 4, but with the full ISI interaction.

was also found by the substantially different calculations of Refs. [14,32].

We consider next the role of the final ηd distortion for the $np \to \eta d$ process at the energies considered. We show in Fig. 4 the results when one includes the final-state interaction. The models with a large ηN scattering length give a good description of the data near threshold. This was already the case for the nonrelativistic case in Ref. [5] (see Fig. 6 therein). The new feature of the relativistic calculation is that the high-energy end is now described by those models. However, they fail to reproduce the shape of the cross section in the intermediate region. The good description of the cross section at the high energy end by models 2–6 is due to the modification of the range and strength parameters for the pion in the dynamical two-body models—and does not happen for models 0 and 1.

We stress that in general the two groups I and II of models studied lead to very similar results for the cross section. This indicates that the failure of all models in describing the data, simultaneously very near and far away from threshold, is not an artifact of the chosen regularization (or cutoff) of the high momenta tail, or of the off-shell behavior of the
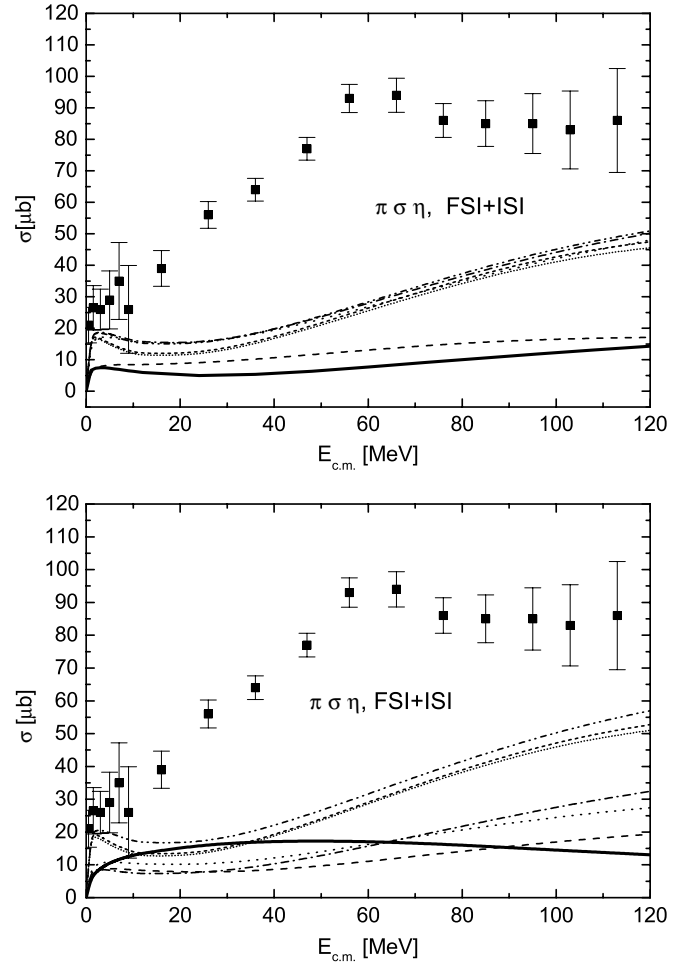
meson-nucleon scattering transition matrix, which cannot be assessed experimentally. The checked independence of the results on that necessarily model-dependent input strengthens the conclusions to be drawn at the end.

Further and more decisive conclusions demand an exact treatment of the initial state reduction effect, which as explained in Ref. [14], may be different for the different meson exchanges. This will be addressed in the next section.

C. The NN initial state interaction

All the results shown in the previous section were obtained with an approximation for the distortion from the NN interaction in the initial state (ISI), more precisely, for the convolution integral of the production amplitude with the scattering transition matrix for the initial NN state. Given the relatively high threshold energy for η production, one may be led to neglect the energy dependent part, i.e., the principle part of that integral. Then the distortion is simply described by a constant factor, originated by the "$i\pi\delta$," or the two nucleon unitarity cut contribution to that integral. However, since different mesons have different ranges, the contribution to the principle part is not the same for all the mesons. Moreover, as explained in Ref. [14], there is a cancellation between the Born

TABLE IV. Reduction factors from the initial state NN interaction in the several models, for the case where the $\pi + \eta + \sigma$ exchanges are present simultaneously.

Model	Reduction factor
0	0.7014
1	0.1739
2	0.1298
3	0.0841
4	0.0874
5	0.0834
6	0.0818

term and the contribution from the unitarity cut. Consequently, the principal part, although small, acquires a leading role in the reduction effect of the cross section.

Therefore, in this section we present in Fig. 5 the results corresponding to Fig. 4, but where the complete initial state distortion is included. The main outcome visible in Fig. 5 is that the models with larger ηN scattering length now also fail in the description of the data for high energy region.
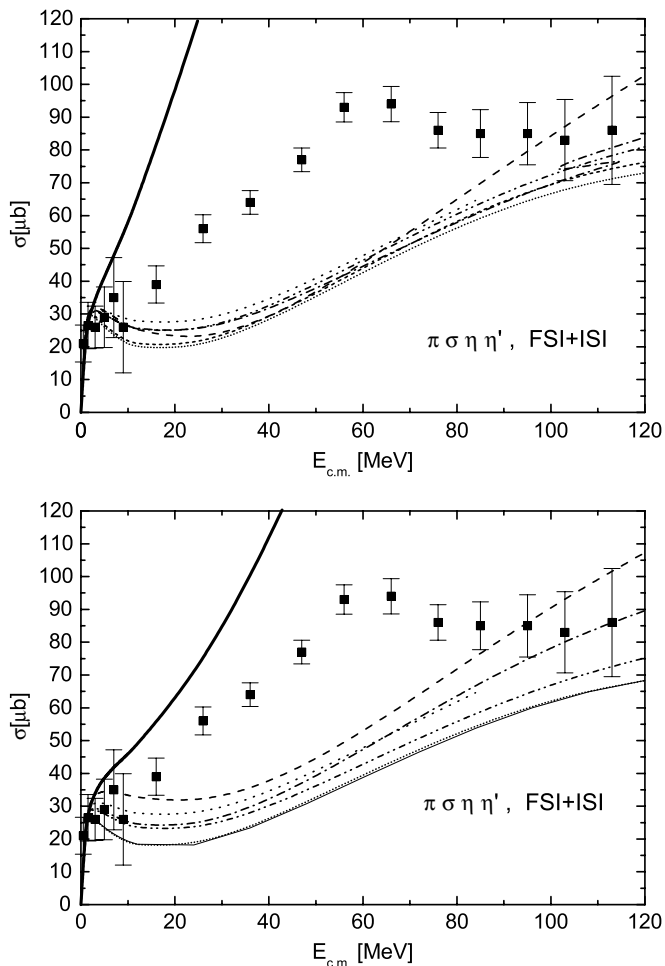

FIG. 6. The same as Fig. 5, but with the inclusion of η' exchange in the box diagram represented by Fig. 1.

We verified that model 0 is the one afected to the least extent by the initial state interaction, as Table IV reports. This finding is consistent with the specific content of that model: the pion momentum range parameter α_π and the scattering length for the short-range ηN interaction are smaller than in other models. Due to this feature, and since the initial state interaction is induced by large three-momentum transfer (short-distance interactions) between the two nucleons, in model 0, both the pion and the heavier mesons are less affected by the initial state reduction.

D. The heavy meson exchange

Finally, we introduced in the box diagram the contribution of the η' meson with its strength adjusted so as to reproduce the cross section near threshold. Since this is a heavy meson exchange, this process acts like a background correction to the isobar model of the nucleon-meson amplitude. Therefore, there is no S_{11} resonance propagation associated to this exchange, but a simple contact or constant term.

The results in Fig. 6 indicate that a reasonable description of the data could be obtained with a model in between model 0 and model 1, i.e., with a ηN scattering length larger than 0.42 fm and smaller than 0.72 fm.

IV. CONCLUSIONS

To summarize, the relativistic calculation of the $np \rightarrow \eta d$ presented here is based on meson exchange production mechanisms and confirms that the final state ηd interaction is very important near threshold, as found before in nonrelativistic models. This interaction alone explains the enhancement effect observed in the cross section near threshold. This result is not surprising since the system has a very strong ηd interaction in the final state and therefore it follows from Watson's theorem [33] that the shape of the cross section will be determined basically by this final-state interaction.

Although the pion exchange visibly does not describe the data near threshold because it needs to be further enhanced by the ηd final state interaction, an important conclusion is that the relativistic pion exchange contribution dominates the reaction exchange mechanisms.

Also, relativistic models corresponding to relatively lower values of the ηd scattering length (e.g., the Julich model, labeled here by model 0) when compared to their nonrelativistic versions, have the large pion momentum range reduced, and simultaneously the small momentum strength accentuated relatively to the high momentum strength. The first feature is important for the energy dependence of the cross section in the threshold region, while the second is important away from the threshold energy region. A fine balance in the combination of the two features seem to be needed to describe successfully the overall energy dependence of the cross section.

Another important conclusion is that the NN initial state interaction cannot be described by the same constant factor for all the meson-nucleon models, due to the accidental cancellation between the undistorted term and the unitarity cut contribution.

Therefore, the control of relativistic effects, as well as of the distortions by initial and final state interactions, is needed in the phenomenological analysis of the reaction. Namely, it may help narrowing the uncertainty in the knowledge of the ηN scattering length. A value for this one between 0.42 (model 0) and 0.72 fm (model 1) seems to be indicated by this study, together with the exchange of a very short-range heavy meson. Nevertheless, our results call for a comprehensive study to search for the ηN model parameters which describe η production, both on the nucleon and on the deuteron, very near as well as away from the threshold energy.

[1] H. Calén *et al.*, Phys. Rev. Lett. **79**, 2642 (1997).

[2] H. Calén *et al.*, Phys. Rev. Lett. **80**, 2069 (1998).

[3] H. Garcilazo and M. T. Peña, Phys. Rev. C **61**, 064010 (2000).

[4] H. Garcilazo and M. T. Peña, Phys. Rev. C **63**, 021001(R) (2001).

[5] H. Garcilazo and M. T. Peña, Phys. Rev. C **66**, 034606 (2002).

[6] N. Kaiser, T. Waas, and W. Weise, Nucl. Phys. **A612**, 297 (1997).

[7] C. Wilkin, Phys. Rev. C **47**, R938 (1993).

[8] M. Batinić, I. Šlaus, A. Švarc, and B. M. K. Nefkens, Phys. Rev. C **51**, 2310 (1995).

[9] M. Batinić, I. Dadić, I. Šlaus, A. Švarc, B. M. K. Nefkens, and T.-S. H. Lee, nucl-th/9703023.

[10] A. M. Green and S. Wycech, Phys. Rev. C **55**, R2167 (1997).

[11] A. M. Green and S. Wycech, Phys. Rev. C **60**, 035208 (1999).

[12] A. Sibirtsev, S. Schneider, Ch. Elster, J. Haidenbauer, S. Krewald, and J. Speth, Phys. Rev. C **65**, 044007 (2003).

[13] W. Grein, A. König, P. Kroll, M. P. Locher, and A. Švarc, Ann. Phys. (NY) **153**, 301 (1984).

[14] V. Baru, A. M. Gasparyan, J. Haidenbauer, C. Hanhart, A. E. Kudryavtsev, and J. Speth, Phys. Rev. C **67**, 024002 (2003).

[15] C. Hanhart, Phys. Rep. **397**, 155 (2004).

[16] W. W. Buck and F. Gross, Phys. Rev. D **20**, 2361 (1979).

[17] F. Gross, J. W. Van Orden, and Karl Holinde, Phys. Rev. C **45**, 2094 (1992).

[18] R. Machleidt, K. Holinde, and C. Elster, Phys. Rep. **149**, 1 (1987).

[19] H. Garcilazo and M. T. Peña, Phys. Rev. C **59**, 2389 (1999).

[20] J.-F. Germond and C. Wilkin, Nucl. Phys. **A518**, 308 (1990); G. Fäldt and C. Wilkin, Phys. Scr. **64**, 427 (2001).

[21] H. Garcilazo, Phys. Rev. C **67**, 055203 (2003).

[22] J. H. Hetherington and L. H. Schick, Phys. Rev. **137**, B935 (1965).

[23] R. A. Arndt, C. H. Oh, I. I. Strakovsky, R. L. Workman, and F. Dohrmann, Phys. Rev. C **56**, 3005 (1997).

[24] R. A. Arndt, I. I. Strakovsky, and R. L. Workman, Phys. Rev. C **62**, 034005 (2000).

[25] H. Zankel, W. Plessas, and J. Haidenbauer, Phys. Rev. C **28**, 538 (1983).

[26] R. Machleidt, Adv. Nucl. Phys. **19**, 189 (1989).

[27] T. A. Rijken, V. G. J. Stoks, and Y. Yamamoto, Phys. Rev. C **59**, 21 (1999).

[28] M. Benmerrouche and N. C. Mukhopadhyay, Phys. Rev. Lett. **67**, 1070 (1991).

[29] L. Tiator, C. Bennhold, and S. S. Kamalov, Nucl. Phys. **A580**, 455 (1994).

[30] S.-L. Zhu, Phys. Rev. C **61**, 065205 (2000).

[31] K. Holinde, Phys. Rep. **68**, 121 (1981).

[32] K. Nakayama, J. Speth, and T.-S. H. Lee, Phys. Rev. C **65**, 045210 (2002).

[33] K. M. Watson, Phys. Rev. **88**, 1163 (1952).